Eur Biophys J (2001) 30: 268–272
DOI 10.1007/s002490100144

ARTICLE

Michael P. Hughes · Hywel Morgan · Frazer J. Rixon

Dielectrophoretic manipulation and characterization of herpes simplex virus-1 capsids

Received: 12 October 2000 / Revised version: 18 January 2001 / Accepted: 18 January 2001 / Published online: 28 March 2001

Abstract The dielectrophoretic behaviour of the capsids of herpes simplex virus type-1 has been measured over a range of conductivities of KCl solutions, with and without the addition of mannitol. The dielectrophoretic response of the capsids was recorded by measuring the frequency corresponding to zero dielectrophoretic force. The data were analysed using a multi-shelled model, and the permittivity and conductivity of the particles estimated. The capsid was modelled as a porous protein shell through which suspending medium passes, an inner chamber containing suspending medium in equilibrium with the outside, and a central core of protein (the scaffold). Capsids suspended in KCl without mannitol exhibited a different behaviour to those suspended in KCl with mannitol.

Keywords Dielectrophoresis · Dielectric properties · Capsid · Electrical double layer

Introduction

Dielectrophoresis (DEP) is the term given to the force acting on a polarizable particle suspended in a spatially non-uniform electric field. This force arises due to the interaction of the non-uniform field and the dipole induced in the particle (Pohl 1978; Jones 1995). The induced dipole moment is a function of the dielectric properties of the particle and the frequency of the applied field.

DEP can either act to move particles towards or away from regions of high electric field strength, termed "positive" and "negative" DEP, respectively. In the case of particles exhibiting one or more dielectric dispersions, both types of behaviour can occur within different frequency windows. For a solid homogeneous particle, and in low suspending medium conductivities, the DEP force changes sign once (generally from positive to negative) at a particular frequency. Measurement of this "zero-force" frequency as a function of the suspending medium conductivity can be used to characterize the dielectric properties of the particle (e.g. Gimsa et al. 1991; Gascoyne et al. 1993; Green and Morgan 1999).

DEP has been used to characterize and manipulate/separate micro-organisms such as yeast (Huang et al. 1992), bacteria (Markx et al. 1994; Hughes and Morgan 1999) and human blood cells (Becker et al. 1995; Chan et al. 2000; Wang et al. 2000) for a number of years. However, the DEP properties of macromolecules (Washizu and Kurosawa 1990; Washizu et al. 1994), latex spheres (Green and Morgan 1997, 1999) and viruses, including influenza (Schnelle et al. 1996), sendai (Müller et al. 1996), tobacco mosaic (Morgan and Green 1997) and herpes simplex (Hughes et al. 1998), have only recently been investigated.

In this work we have investigated the dielectrophoretic properties of the capsids of herpes simplex virus type-1 (HSV-1). This virus has a more complex, multi-layered structure than many viruses, and in some respects is similar to a simple mammalian cell, consisting of a conducting core surrounded by an insulating membrane. The complete particle, or *virion*, is encased in an envelope consisting of a lipid bilayer with embedded glycoproteins. Inside this is a thick, relatively low-density, amorphous protein layer called the tegument, which in turn surrounds the capsid containing the viral DNA (Whitley 1996). A complete diagram of the structure is shown in Fig. 1. The icosahedral capsid is a robust protein shell with a mean thickness of 15 nm and

M.P. Hughes[1] · H. Morgan (✉)
Bioelectronic Research Centre,
University of Glasgow, Glasgow G12 8QQ, UK
E-mail: h.morgan@elec.gla.ac.uk
Tel.: +44-141-3305237
Fax: +44-141-3304907

F.J. Rixon
MRC Virology Unit, University of Glasgow,
Glasgow G11 5JR, UK

Present address:
[1]Biomedical Engineering Group,
University of Surrey, Guildford, Surrey GU2 5XH, UK

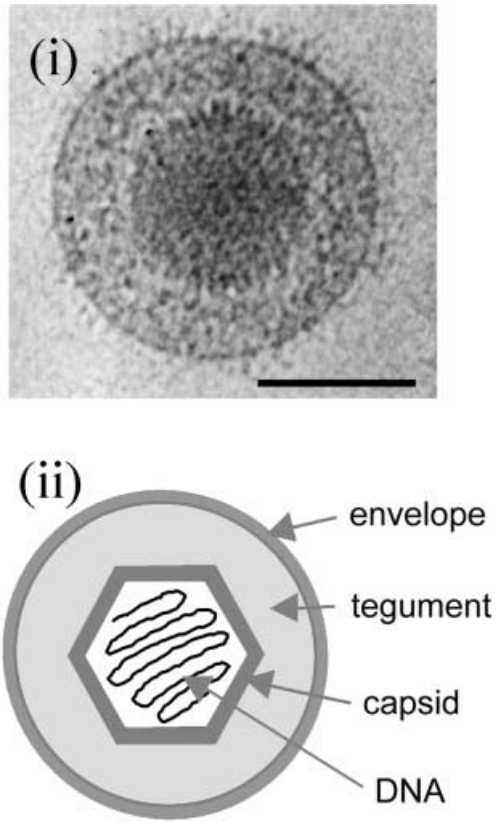

Fig. 1 *Top* A transmission electron cryo-micrograph of a frozen hydrated herpes simplex virus, type 1 (HSV-1) particle, provided by W. Chiu, Baylor College of Medicine. *Bottom* Schematic representation of the HSV-1 virion showing the locations of the DNA (not visible in the primary image), capsid, tegument and envelope. The scale *bar* represents 100 nm

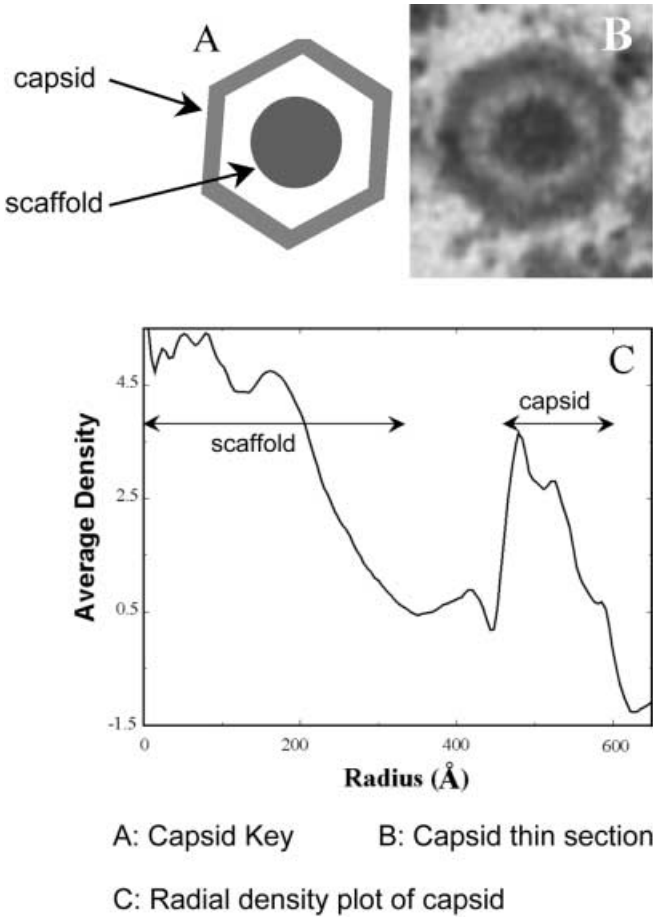

Fig. 2A–C Radial density distribution of the HSV-1 B capsid. **A** Schematic representation of an HSV-1 B capsid showing the positions of the capsid shell and the scaffold. **B** A transmission electron micrograph of a thin section through an HSV-1 capsid. The other shell is clearly visible as a dark region about the periphery, whilst the scaffolding proteins appear as a dark mass around the centre of the capsid. **C** Mean radial density distribution of the B capsid derived from a computer-generated three-dimensional reconstruction of purified B capsids. Note the low density separating the scaffold and the capsid shell. Panel **C** is reproduced from Zhou et al. (1999)

an overall diameter of 125 nm. The viral DNA enters the pre-formed capsid through holes of approximately 5 nm diameter, which (in this study) allow access of the suspending medium into the interior of the capsid.

Capsids can be harvested prior to the addition of the tegument and envelope (Zhou et al. 1998), thus enabling their properties to be measured independently of other viral components. Three forms of the capsid can be isolated and are referred to as A (comprising only the capsid shell with no internal electron density), B (in addition to the capsid shell there is an internal protein core, the scaffold, which is needed during capsid assembly) and C (containing the viral DNA in place of the internal scaffold). The work presented in this paper was performed using B capsids. The fine structure of the B capsid has been studied by electron cryomicroscopy and computer reconstruction imaging (Zhou et al. 1994, 1998), and a diagram showing the structure and average density of the capsid is reproduced in Fig. 2 (from Zhou et al. 1999). In this paper the DEP behaviour of B capsids has been measured over a range of conductivities, in solutions of KCl and KCl containing 280 mM mannitol. The behaviour of the capsids was modelled to obtain estimates of the dielectric properties of the particles.

Materials and methods

Capsid preparation

Capsids were prepared using the protocol described in Zhou et al. (1998). Capsids were harvested from baby hamster kidney cells infected with HSV-1 at 5 pfu/cell at 37 °C for 16 h. B capsids were then fluorescently labelled using rhodamine (Sigma). Fluorescent labelling was performed according to the following protocol. A 10 mL solution containing rhodamine (10 mM) and *N*-hydroxysuccinimide (10 mM) was prepared, and its pH adjusted to 4.75 with NaOH. To this solution, 9.6 mg of 1-ethyl-3-(3-dimethylaminopropyl)carbodiimide was added with stirring. The pH of this reaction was monitored, and HCl was added to maintain a pH of 4.75. When the pH became stable, 10 mL of the solution was added to 2.4 mL of 0.1 M triethanolamine (TEA) buffer (pH 7.0) to produce the labelling solution. Then 0.5 mL of the labelling solution was mixed with 0.5 mL of capsids in 0.4 M TEA buffer (pH 7.0) and mixed overnight at room temperature. The capsids

were pelleted at 20,000 rpm in a Beckman TLA 100.2 rotor, washed, then resuspended in either ultra-pure water or 280 mM mannitol solution, which is used to produce iso-osmotic suspending media. A sample was examined by electron microscopy to ensure that the capsids had retained their integrity during the labelling procedure. Shortly prior to experimentation, aliquots of the capsid solution were added to KCl solutions of various ionic strengths. A range of solution conductivities, from 0.25 to 160 mS m^{-1} at 10 points per decade, was used.

Microelectrodes

Electrodes were fabricated on glass microscope slides using standard photolithographic methods. A 100 nm thick layer of Au was evaporated on top of a 10 nm Ti seed layer. The electrodes were of the polynomial design (Huang and Pethig 1991), with a gap of 2 μm between adjacent electrodes and a 6 μm gap across the centre. A micro-litre volume chamber was constructed around the electrode using Perspex spacers and adhesives. The chamber had a depth of approximately 50 μm and a sample volume of the order of 1 μL. For the experiments, the capsid solution was pipetted into the chamber and the assembly sealed with a cover slip.

Experimental

The electrodes were powered using a Hewlett-Packard signal generator providing 10 V peak-to-peak sinusoidal signals over the frequency range 1 kHz to 20 MHz. Potentials were applied to give a 180° phase difference between adjacent electrodes. Experiments were observed using a Nikon Microphot microscope with Texas Red filter block (dichroic mirror wavelength 580 nm) and camera attachment. Conductivity measurements were performed using a Hewlett-Packard 4192A impedance analyser and a Sentek conductivity cell in the range 100 kHz to 1 MHz.

Results

In solutions of low conductivity (either KCl or KCl + mannitol, below 0.5 mS m^{-1}), capsids exhibited positive DEP at low frequencies and negative DEP at high frequencies. A point of zero force (corresponding to the transition from positive to negative DEP) occurred at a frequency of approximately 3–4 MHz. Single particles were clearly visible, and the zero-force or crossover frequencies could be accurately determined for each particle. Aggregates of capsid were rarely seen; the presence of single capsids was confirmed by comparison with single fluorescent latex spheres of a similar size. Owing to the low level of fluorescence signal we were unable to photograph capsid movement with our current experimental system. The error in the zero-force measurements was very small; error bars are typically of the size of a single symbol and are therefore not shown. A narrow distribution in crossover frequencies was measured, indicating that all of the particles are nearly identical. In general, as the suspending medium conductivity was increased, the crossover frequency also increased.

Figure 3 shows the variation in crossover frequency plotted as a function of the suspending medium conductivity. The data shown in the figures was for a total of three separate capsid preparations. The distribution between populations was very small and is not shown on the figures. Figure 3a shows data for KCl + 280 mM mannitol solutions, where the crossover frequency is seen to increase with medium conductivity, with a maximum in crossover frequency at 13 MHz, corresponding to a conductivity of 10 mS m^{-1}. Above this conductivity, the crossover frequency decreased rapidly to approximately 250 kHz for a solution conductivity of 16 mS m^{-1}. For KCl without mannitol, the crossover frequency increased by nearly one decade (to 20 MHz, the maximum frequency from our signal generator) for a decade change in conductivity as shown in Fig. 3b. At this frequency, and in electrolytes of conductivity greater than 2 mS m^{-1}, the capsids exhibited only positive DEP for all the measured electrolyte conductivities (up to 160 mS m^{-1}).

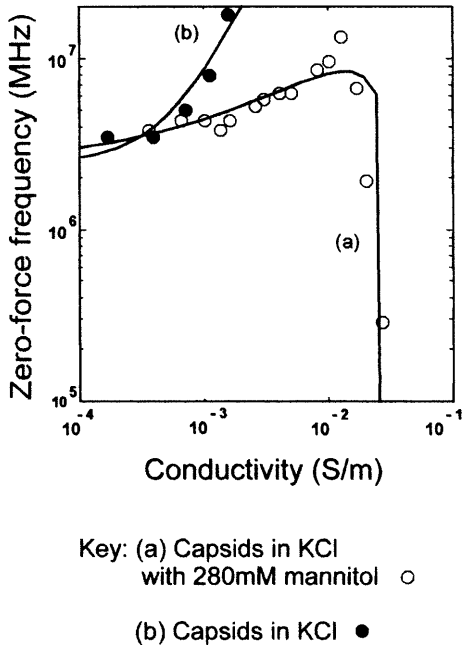

Fig. 3 Plot of the zero-force data for capsids in KCl of varying conductivity. The data in (*a*) are with the addition of 280 mM mannitol, whilst in (*b*) the suspending medium consists solely of KCl solution. *Circles* indicate the measured crossover frequency for a given suspending medium conductivity; *lines* indicate the best fit to the data with dielectric parameters detailed in the text

Discussion

Recent work has shown that measurements of the crossover or zero-force frequency can be used to analyse the dielectric properties of sub-micrometre particles (e.g. Green and Morgan 1999). For example, assuming that the particles are either solid homogeneous spheres (Green and Morgan 1999) or rods (Morgan and Green 1997), values for the surface conductance and permittivity of the particle can be obtained. In this work we have used similar models to analyse the dielectrophoretic behaviour of the capsids.

The structure of the capsid is shown in Figs. 1 and 2. The outer shell of the capsid contains channels (Zhou et al. 1998), which allow the free movement of ions in and out of the capsid interior. Similarly, the scaffold is a porous structure with a complex geometry. Although these structures are elaborate, a first approximation can be made by modelling the capsids as solid homogeneous particles (such as latex spheres). Using this model the experimental data for the capsids in KCl + mannitol data can be analysed.

It has been shown that the dielectrophoretic properties of particles are heavily influenced by a surface conductance (Arnold and Zimmermann 1988; Green and Morgan 1997, 1999), where the particle conductivity is given by:

$$\sigma_p = \sigma_{pbulk} + \frac{2K_s}{r} \quad (1)$$

In this expression, K_s is the surface conductance and σ_{pbulk} is the bulk conductivity of the particle of radius r. Owing to the dependence of conductivity with inverse radius of the particle, the influence of surface conductance becomes greater as the particle size is reduced. Thus, for a sub-micrometre particle, surface conductance effects tend to dominate the dielectrophoretic properties.

A refinement of this surface conductance model (Lyklema 1995; Hughes et al. 1999) involves dividing the total surface conductance into two components: a contribution due to ion movement in the Stern layer (K_s^i) and a second due to ion movement in the diffuse part of the electrical double layer (K_s^d). The total particle conductivity is then:

$$\sigma_p = \sigma_{pbulk} + \frac{2K_s^i}{r} + \frac{2K_s^d}{r} \quad (2)$$

Analysis shows that the Stern layer conductance is dominated by the surface charge density of the particle and the diffuse layer conductance depends on the zeta potential (the potential at the slip plane) and the suspending medium conductivity. At low suspending medium conductivities the contribution from the diffuse layer is very small, so that the surface conductance of the particle is dominated by charge movement in the Stern layer (Lyklema 1995; Hughes et al. 1999).

The solid line in Fig. 3a shows a best fit to the data calculated with a particle permittivity $\epsilon_p = 70$, Stern layer surface conductance $K_s^i = 0.2$ nS and zeta potential = 75 mV. The suspending medium conductivity is plotted along the x-axis (with the suspending medium permittivity $\epsilon_m = 78$). Although this data does fit the experimentally measured zero-force frequencies, the high value of internal permittivity required for a fit ($\epsilon_p = 70$) means that the magnitude of the negative part of the Clausius-Mossotti factor is very small at high frequencies. This value is unrealistic since it would not be sufficient to produce the degree of negative DEP force seen on the particles at high frequencies. Therefore it can be concluded that this simple model does not accurately reflect the properties of the particles.

The model of the capsid can be extended by approximating it to a series of concentric shells (Hanai et al. 1975). In such a model the capsid would comprise an outer protein shell, on average 15 nm thick (inner radius 47.5 nm), comprising a structured network of protein molecules, having channels of up to 5 nm diameter (Zhou et al. 1994, 1998). These channels connect the interior and exterior of the capsid so that the internal space is equivalent to a chamber full of suspending medium. At the centre of the capsid are the scaffolding proteins, which we have treated as a solid protein sphere (60 nm diameter). Using this shell model a more realistic fit to the data was obtained. The best fit in this case was with a particle internal permittivity $\epsilon_p = 30$, an internal conductivity $\sigma_p = 30$ mS m^{-1}, shell permittivity = 60, $K_s^i = 0.15$ nS and zeta potential = 95 mV. This fit is shown by the same solid line in Fig. 3a. This more complete model predicts a high-frequency limit for the Clausius-Mossotti factor of –0.2 (a value which could result in a force capable of producing the observed movement). However, unlike the case of the homogeneous particle, it is not possible to obtain a unique fit to the zero-force versus conductivity data for the shell model, so that this parameter set is not unique.

The behaviour of capsids suspended solely in KCl (without mannitol) was quite different, as shown in Fig. 3b. The data show a rapid increase in crossover frequency over a very small window of increasing suspending medium conductivity, data which cannot be accounted for by any of the simple models. The reasons for this are not clear at present, but possible explanations may relate to the porous nature of the shell and scaffold. The experimental data can be accounted for by including an internal conductivity which is proportional to the square of the medium conductivity (as indicated by the curve in Fig. 3b), but at present we have no justification for this approach.

Mannitol is a sugar of molecular weight 182.2, and is used as a non-metabolizing molecule to maintain osmolality in electrokinetic experiments on cells. It is non-polar and reduces the permittivity of the suspending medium by 0.7 units (Arnold et al. 1993). The reason for its effect on the behaviour of the capsids is unclear. It does not cause aggregation of the particles: in all experiments individual capsids could be clearly seen. The reasons for the discrepancy in the data for a suspending medium with and without mannitol are currently the subject of ongoing investigations.

Conclusions

The dielectrophoretic manipulation of herpes simplex virus-1 capsids has been achieved in solutions of KCl and KCl + mannitol. Measurements of the zero-force (or crossover) frequency have been made as a function of medium conductivity and the spectra analysed in terms

of interfacial relaxation mechanism. The addition of mannitol to the suspending medium greatly alters the observed dielectrophoretic response of the capsids, which we postulate may be due to the mannitol reducing the surface charge density of the capsid.

Acknowledgements The authors would like to thank Mary Robertson for electrode fabrication, Joyce Mitchell for capsid preparation and Sharon Hardie for developing the labelling procedure.

References

Arnold WM, Zimmermann U (1988) Electro-rotation: development of a technique for dielectric measurements on individual cells and particles. J Electrostat 21:151–191

Arnold WM, Gessner AG, Zimmermann U (1993) Dielectric measurements on electro-manipulation media. Biochim Biophys Acta 1157:32–44

Becker FF, Wang X-B, Huang Y, Pethig R, Vykoukal J, Gascoyne PRC (1995) Separation of human breast cancer cells from blood by differential dielectric affinity. Proc Natl Acad Sci USA 92:860–864

Chan KL, Chan KL, Morgan H, Morgan E, Cameron IT, Thomas MR (2000) Measurements of the dielectric properties of lymphocytes and trophoblast cells using AC electrokinetic techniques. Biochim Biophys Acta 1500:313–322

Gascoyne PRC, Pethig R, Burt JPH, Becker FF (1993) Membrane-changes accompanying the induced-differentiation of friend murine erythroleukemia-cells studied by dielectrophoresis. Biochim Biophys Acta 1149:119–126

Gimsa J, Marszalek P, Löwe U, Tsong TY (1991) Dielectrophoresis and electrorotation of neurospora slime and murine myeloma cells. Biophys J 60:749–760

Green NG, Morgan H (1997) Dielectrophoretic separation of nano-particles. J Phys D 30:L41–L44

Green NG, Morgan H (1999) Dielectrophoresis of submicrometer latex spheres. 1. Experimental results. J Phys Chem 103:41–50

Hanai T, Koizumi N, Irimajiri A (1975) A method for determining the dielectric constant and the conductivity of membrane-bounded particles of biological relevance. Biophys Struct Mech 1:285–294

Huang Y, Pethig R (1991) Electrode design for negative dielectrophoresis. Meas Sci Technol 2:1142–1146

Huang Y, Hölzel R, Pethig R, Wang X-B (1992) Differences in the ac electrodynamics of viable and nonviable yeast-cells determined through combined dielectrophoresis and electrorotation studies. Phys Med Biol 37:1499–1517

Hughes MP, Morgan H (1999) Measurement of bacterial motor force by negative dielectrophoresis. Biotechnol Prog 15:245–249

Hughes MP, Morgan H, Rixon FJ, Burt JPH, Pethig R (1998) Manipulation of herpes simplex virus type 1 by dielectrophoresis. Biochim Biophys Acta 1425:119–126

Hughes MP, Morgan H, Flynn MF (1999) The dielectrophoretic behaviour of sub-micron latex spheres: influence of surface conductance. J Colloid Interface Sci 220:454–457

Jones TB (1995) Electromechanics of particles. Cambridge University Press, Cambridge

Lyklema J (1995) Fundamentals of interface and colloid science. Academic Press, London

Markx GH, Huang Y, Zhou X-F, Pethig R (1994) Dielectrophoretic characterization and separation of microorganisms. Microbiology 140:585–591

Morgan H, Green NG (1997) Dielectrophoretic manipulation of rod-shaped viral particles. J Electrostat 42:279–293

Müller T, Fiedler S, Schnelle T, Ludwig K, Jung H, Fuhr G (1996) High frequency electric fields for trapping of viruses. Biotechnol Tech 10:221–226

Pohl HA (1978) Dielectrophoresis. Cambridge University Press, Cambridge

Schnelle T, Müller T, Fiedler S, Shirley SG, Ludwig K, Hermann A, Fuhr G (1996) Trapping of viruses in high-frequency electric field cages. Naturwissenschaften 83:172–176

Wang X-B, Yang J, Huang Y, Vykoukal J, Becker FF, Gascoyne PRC (2000) Cell separation by dielectrophoretic field-flow-fractionation. Anal Chem 72:832–839

Washizu M, Kurosawa O (1990) Electrostatic manipulation of DNA in microfabricated structures. IEEE Trans Ind Appl 26:1165–1172

Washizu M, Suzuki S, Kurosawa O, Nishizaka T, Shinohara T (1994) Molecular dielectrophoresis of biopolymers. IEEE Trans Ind Appl 30:835–843

Whitley RJ (1996) Herpes simplex viruses. In: Fields BN, Knipe DM, Howley PM (eds) Fields virology. Lippincott-Raven, Philadelphia, pp 2297–2342

Zhou ZH, Prasad BVV, Jakana J, Rixon FJ, Chiu W (1994) Protein subunit structures in the herpes-simplex virus a-capsid determined from 400-kv spot-scan electron cryomicroscopy. J Mol Biol 242:456–469

Zhou ZH, MacNab SJ, Jakana J, Scott LR, Chiu W, Rixon FJ (1998) Identification of the sites of interaction between the scaffold and outer shell in herpes simplex virus-1 capsids by difference electron imaging. Proc Natl Acad Sci USA 95:2778–2783

Zhou ZH, Chen DH, Jakana J, Rixon FJ, Chiu W (1999) Visualization of tegument-capsid interactions and DNA in intact herpes simplex virus type 1 virions. J Virol 73:3210–3218